MAGNETIC RESONANCE IN MEDICINE 3, 454–462 (1986)

Projection Angiograms of Blood Labeled by Adiabatic Fast Passage

W. THOMAS DIXON,* LEILA N. DU,* DAVID D. FAUL,† MOKHTAR GADO,* AND SUSAN ROSSNICK†

*Mallinckrodt Institute of Radiology, St. Louis, Missouri 63110, and †Siemens Medical Systems, Iselin, New Jersey 08830

Received January 17, 1986; revised February 21, 1986

A surface coil on the neck causes adiabatic fast passage in blood as it flows by through a magnetic field gradient. This allows separation of blood and stationary tissue images of the head. Coronal and sagittal images of a volunteer are presented showing the vertebral and common, internal and external carotid arteries in projection views.

Projection images, that is, images with voxels going all the way through the patient, are convenient for examining arteries because arteries do not stay in one plane for any great distance. Vascular contrast is much more important in projection images than in tomographic images because projection images have larger brightness variations, ruling out narrow window settings. Furthermore arteries are obscured by detail in overlying organs. Ideally stationary tissue should be either shifted out of the artery image or suppressed altogether (*1*).

Any technique which enables separation of moving tissue (blood) from stationary tissue is therefore desirable (*2–4*). We use an adiabatic fast passage (*5, 6*). In this technique an rf field above (below) the Larmor frequency is turned on; the main field is increased (decreased) until the Larmor frequency rises above (below) the rf frequency; finally the rf is shut off. This procedure reverses the magnetization of the spins.

In a spin's eye view of our experiment, flow turns the rf on then off again by moving the blood spins toward, then away from a small coil on the neck. The important change in Larmor frequency is brought about by moving the spins along a field gradient, along the long axis of the body. Figure 1 illustrates this. Since we rely on natural blood flow to do all this moving, blood magnetization is reversed while stationary tissue is not affected except in a small, smile shaped region of the neck.

Conditions for an adiabatic fast passage are that

$$H_1/D \ll G \ll H_1^2/V$$

where H_1, G, D, and V are rf field strength, magnetic field gradient, auxiliary coil length, and blood velocity, all in consistent units.

The resulting inversion washes downstream a distance of at least VT_1 (*7–9*) so the artery distal to the inversion can be imaged. Figure 2 shows the pulse sequence used

0740-3194/86 $3.00

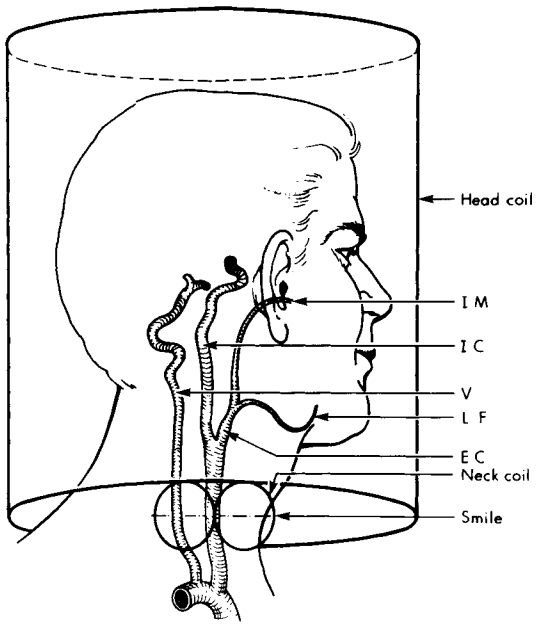

FIG. 1. Blood labeling. The standard head coil is used for transmitting and receiving. The neck coil provides the rf for the adiabatic fast passage. Besides producing the inversion in blood it saturates a region of spins in stationary neck tissue. This region is visible in images as a "smile." The images show blood vessels downstream from the smile. EC, external carotid artery; V, vertebral artery; IC, internal carotid artery; IM, internal maxillary artery.

for imaging. The nonselective 90° pulse following the R wave by 40 ms, our minimum delay, excites the entire head. The read gradients and the nonselective 180° pulse produce Hahn and gradient echoes 25 ms later, in the middle of a 7.7-ms acquisition.

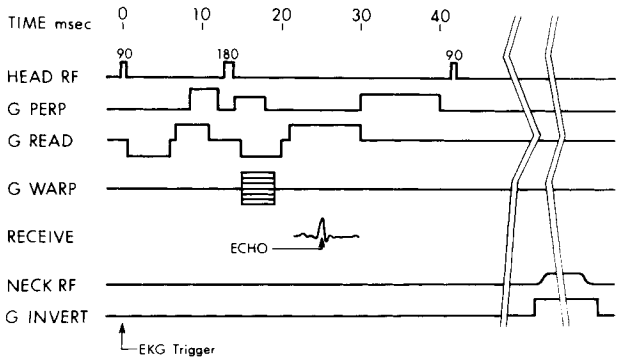

FIG. 2. Pulse sequence. The standard head coil was used for both 90 and 180° pulses and for the receiver. An auxiliary coil was used for "neck rf." The read and invert gradients were along the H_0 axis, the long axis of the subject. The warp axis was horizontal for coronal views and vertical for sagittals. (The subject is supine.) The remaining gradient, G PERP, is orthogonal to the other two.

The read gradient is tailored so that the first moment of the portion between the 90° pulse and the gradient echo is zero. For moment calculations, a 180° pulse is assumed to reverse the contribution of all gradients occurring before that pulse. The gradient echo occurs when the integral of the read gradient (its zero moment) is zero. This precaution makes the phase of the signal independent of velocity (but not of acceleration, jerk, etc.) (*4*). This prevents darkening of blood by phase cancellation within a voxel and confusion of position by a change in the patient's blood flow during the examination.

The two unequal perpendicular gradient pulses close to the 180° pulse have several functions. Since dynamic range problems are worse in projection than in tomographic imaging, we added a perpendicular gradient to reduce the signal. With such a gradient twisting the magnetization, a pixel's brightness varies sinusoidally with object thickness rather than continuing to increase linearly. Objects with a certain thickness or multiples thereof disappear altogether. We used values from 3 to 6 cm for this thickness. Since arteries are less than a centimeter in diameter they are not significantly affected when viewed crosswise but heads are darkened greatly. In principle because of this gradient, the phase of an artery in an image gives its position along the third dimension. We are actually doing three-dimensional imaging but we have not yet tried to interpret the phase. Finally the perpendicular gradient pulse (twister) was broken into two unequal pieces because we had trouble getting good images when a 180° pulse occurred near a gradient echo. (Note that in our pulse sequence the positive and negative read gradients which precede the 180° pulse nearly cancel each other.) Twisting the spins about the third axis then untwisting them after the pulse solved this problem.

The phase-encoding gradient is not turned on immediately following the excitation pulse as in most imaging cycles, but is delayed until immediately before signal acquisition to minimize image distortion due to flow along the phase-encoding direction (*10, 11*).

The long perpendicular gradient and following 90° pulse spoil any remaining transverse and longitudinal magnetization.

Immediately following the spoiler an inversion gradient of 40 s^{-1} cm^{-1} is turned on, rf is applied to the neck coil, the rf is shut off, then the gradient is shut off. These are turned off just before the next *R* wave is anticipated from the heart, then the imager waits for the *R* wave. All the blood passing the coil while the rf is on becomes labeled. The longest possible labeling time is used consistent with the number of cardiac cycles chosen for TR. It is important to turn the rf on and off slowly to prevent saturation of stationary tissue near the neck coil.

Determining the Larmor frequency of spins just under the neck coil is difficult. In general, the neck coil is not centered at the null of the gradient coils, the null of the gradient coil does not coincide with either the center of the image nor the center located by the patient table cross hairs, and furthermore the mere presence of the patient produces susceptibility gradients with strengths comparable to the inversion gradient we used. To determine the Larmor frequency, we use an ungated 0.3-s TR version of the pulse sequence program and look for the "smile" of saturated spins in the resulting image. The smile moves with neck coil frequency and is much easier to

see if a bright copper-doped gel phantom is placed along the coil. After the rf had been set to the Larmor frequency at the coil, we removed this phantom without regard to additional perturbation of the field.

Although the neck coil uses much lower power than the head coil, its power is confined to a smaller volume and it runs at a duty cycle near 50% instead of 5%. Care must be taken not to heat the subject locally. We were able to stay below the ANSI guideline (ANSI C95.1-1982) of 8 W/kg and the FDA guideline of 2 W/kg. Because of the geometry of our coil the former is probably more relevant (*12*).

Power is applied to the neck coil only on alternate acquisitions. The result of this depends on signal averaging. If only one signal average is used the phase of the blood signal varies by an extra 180° every acquisition. This is equivalent to one-half a screen

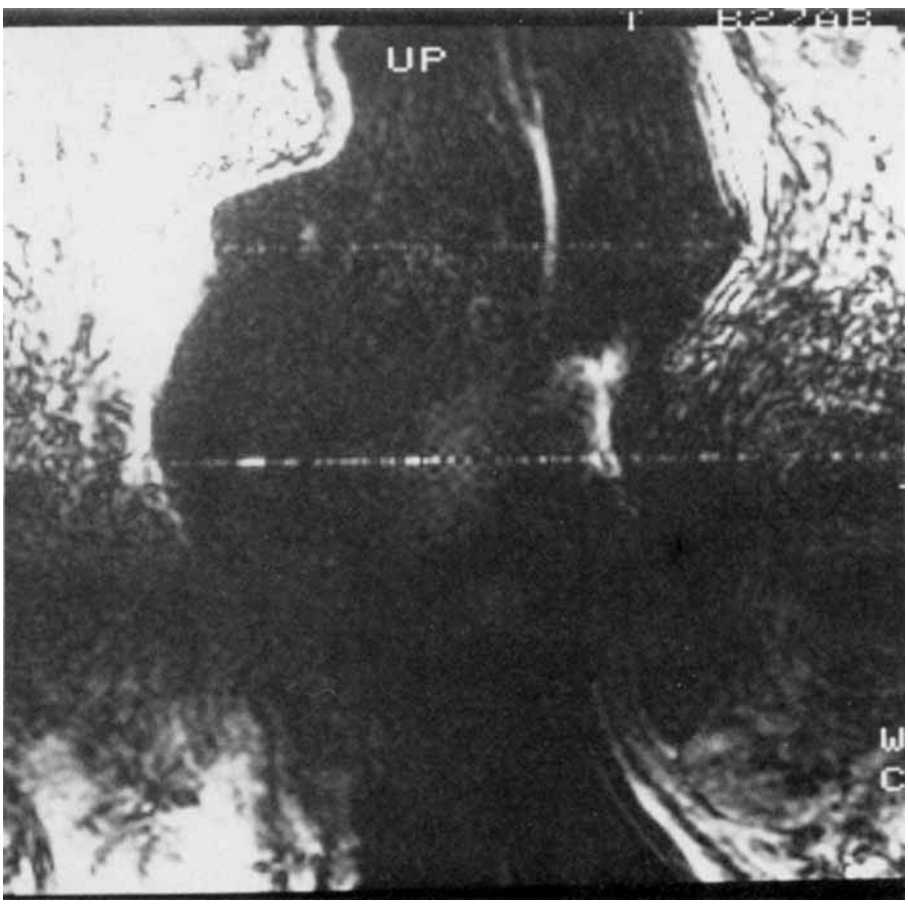

FIG. 3. Sagittal projection showing flowing blood separated from stationary tissue. Technical parameters: trigger every heart beat, 128 × 128 matrix, 2 min acquisition time.

width in the phase-encoding direction. Figure 3 shows the arteries moved out of the body as a result of this. Alternatively, taking two averages, either the blood signal or the stationary tissue signal can be made to cancel. If alternate scans are added and subtracted from memory, or if the sign of the 90° pulse is alternated (but not both) the blood signal alone will be preserved.

These experiments were done on a Siemens Magnetom imager. The Magnetom uses a 1-m superconducting Oxford magnet running at 1.5 T (64 MHz). The imager was triggered by a Siemens Sirecust 400 EKG.

Figure 4 is a block diagram of the additional hardware used. We recommend a low-power rf amplifier for safety reasons. The function generator is set to produce a haversine with enough dc offset so that only the beginning and end of the waveform are negative. This along with the nonlinear behavior of the Mini-Circuits devices gives rf pulses with tapered ends.

The coil is a figure eight of No. 10 insulated wire. The loops are elliptical about 4 × 5 cm, longer in the direction of blood flow. One-half wavelength of RG-58/U coaxial cable is attached and the excess ground braid is spread out radially from the center of the eight and the strands are wrapped 270° around the insulation of the No. 10 wire. The coil is tuned and matched by two 30-pF variable capacitors at the end of the cable. Q is 40–50. The figure-eight shape was chosen to allow labeling of arteries selectively on one side of the neck only and to protect the low-power amplifier output from inductive coupling to the high-power transmitter. The Faraday shield made from the braid protects the amplifier from capacitive coupling.

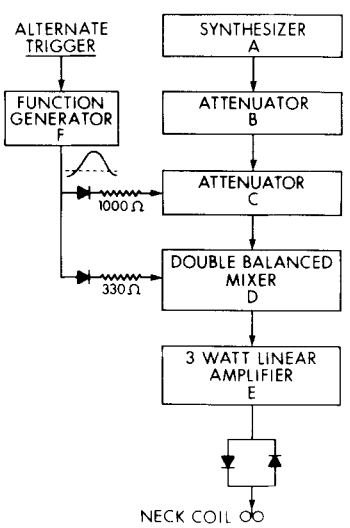

FIG. 4. Block diagram of supplementary hardware which provides rf for adiabatic fast passages. (A) Programmed Test Sources (Littleton, Mass.) PTS160; (B) Wavetek (Beech Grove, Ind.) 5080.1; (C) Mini-circuits (Brooklyn, N.Y.) ZAS-1; (D) Mini-circuits ZAD-3; (E) Electronic Navigation Industries (Rochester, N.Y.) 403LA; (F) Wavetek (San Diego, Calif.) 21.

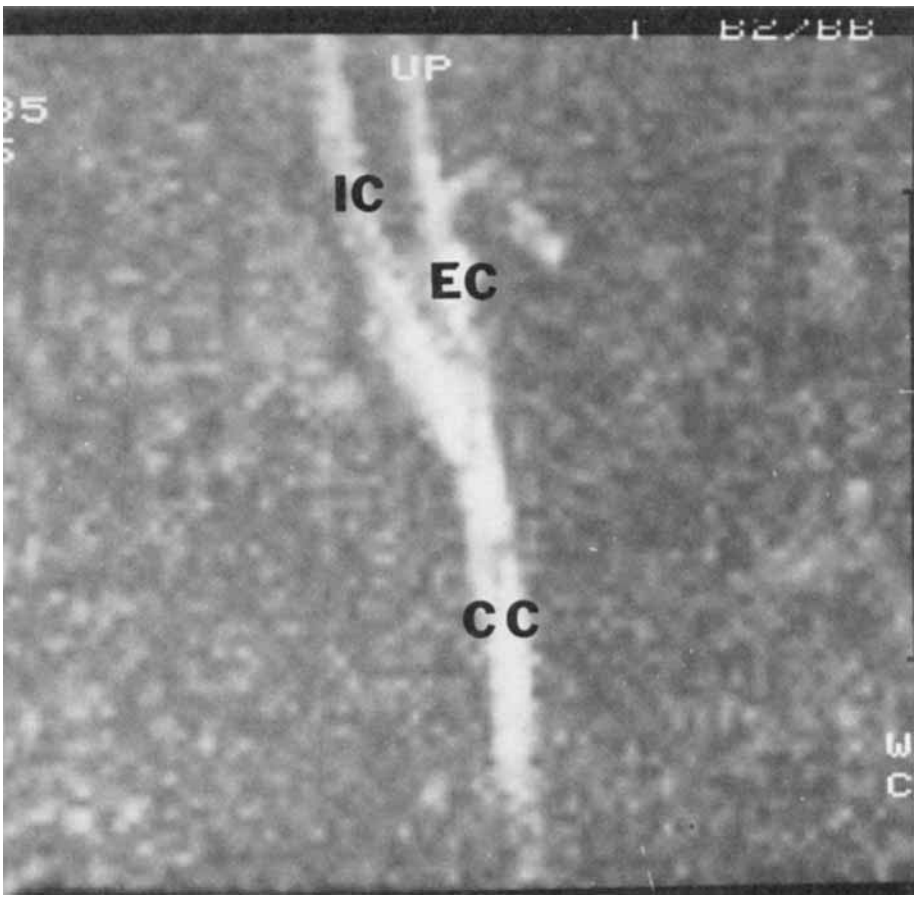

FIG. 5. A projection in sagittal orientation generates an image similar to the lateral view of the arteriogram familiar to radiologists. By placing the auxillary neck coil low enough, the carotid bifurcation is included, which is an important clinical requirement in radiologic evaluation of cerebrovascular occlusive disease. Technical parameters: trigger every heart beat, cropped from 256 × 256 matrix, 4 min acquisition time. CC, common carotid artery; EC, external carotid artery; IC, internal carotid artery.

We demonstrate this technique using the head and neck because the anatomy is favorable and because NMR for intracranial applications has received wide acceptance. Four arteries carry blood to the brain. These arteries, the vertebrals and carotids are fairly superficial in the neck allowing easy labeling, and they have rapid flow reaching the skull in a small number of relaxation times, T_1. Each internal carotid artery irrigates one cerebral hemisphere while the vertebral arteries supply the brain stem and cerebellum.

The most common site of cerebrovascular occlusive disease is the carotid bifurcation in the neck. By placing the coil low enough on the neck, one ensures imaging this region (Fig. 5). Atheromatous *narrowing* of the artery at this location is amenable to

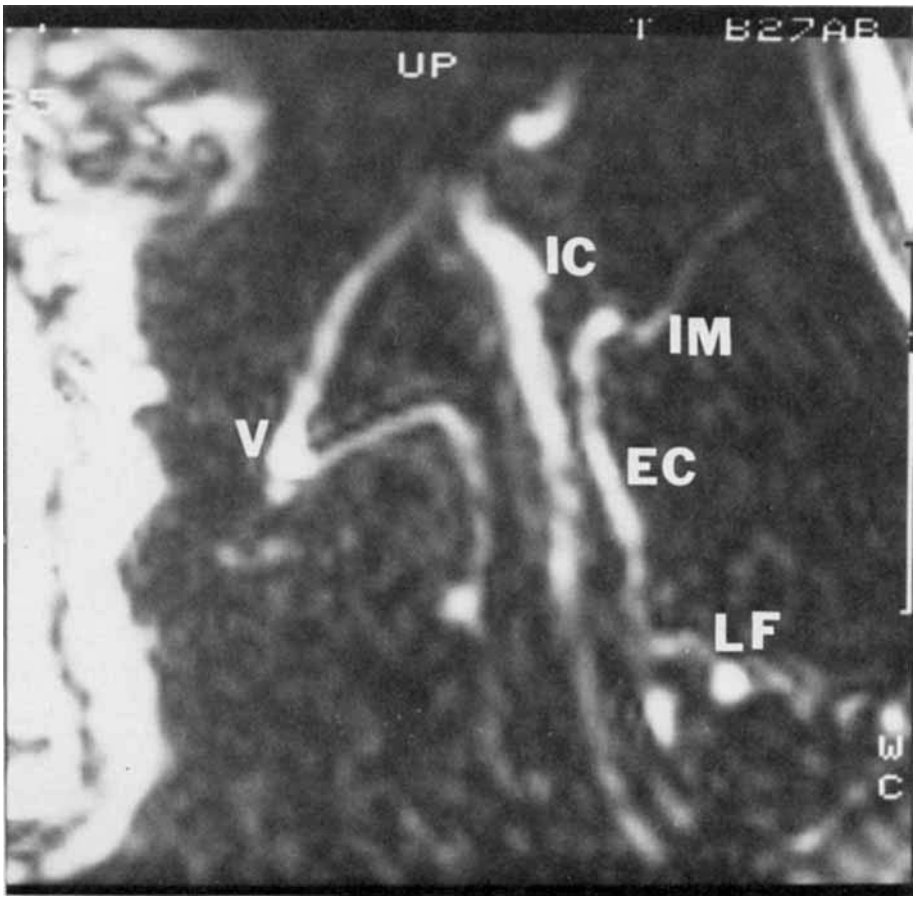

FIG. 6. A projection in sagittal orientation. Triggering every second heart beat allows labeled blood to reach more peripheral vessels. Technical parameters: trigger every 2 heart beats, cropped from a 128 × 128 matrix, 4 min acquisition time. LF, lingual and/or facial artery; EC, external carotid artery; IC, internal carotid artery; V, vertebral artery; IM, internal maxillary artery.

surgical correction since its subcutaneous location is accessible. When narrowing progresses to *complete occlusion,* a different and more involved surgical procedure is indicated. This entails opening the cranial wall and establishing a bypass anastomosis between the extracranial and intracranial arteries.

Therefore prior to treatment planning, it is essential to establish among other things two important facts: (a) whether the artery is narrowed or completely occluded, and (b) whether the location of the narrowing is accessible to surgery.

Figure 6 shows the value of a longer labeling period allowed by triggering every other heart beat instead of every one. More peripheral vessels are made visible. Figure 7 shows a coronal projection.

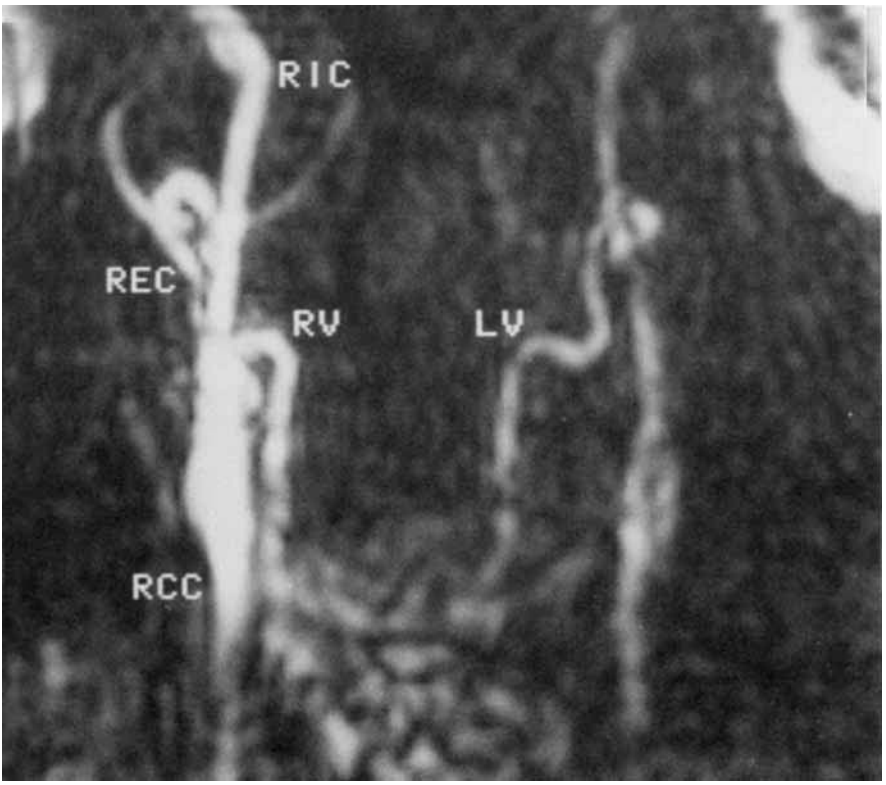

FIG. 7. A projection in coronal orientation generates an image similar to the antero-posterior view of the arteriogram familiar to radiologists. In this experiment a coil was placed on the right side of the neck only. Some labeling occurred in the left vessels also. Technical parameters: Trigger every heart beat, cropped from a 128 × 128 matrix, 2 min acquisition time. RCC, right common carotid artery; RIC, right internal carotid artery; REC, right external carotid artery; RV, right vertebral artery, LV, left vertebral artery.

Traditionally this information has been obtained by performing cerebral arteriography, an invasive procedure requiring puncturing of a vessel, intravascular navigation and the injection of radio-opaque pharmaceutical (contrast material) followed by rapid sequence X-ray radiography. This procedure entails calculated risks related to each of its three components. The NMR technique presents none of these risks.

ACKNOWLEDGMENT

Part of this work was supported by the Whitaker Foundation, Camp Hill, Pennsylvania.

REFERENCES

1. V. J. WEDEEN, R. A. MEULI, R. R. EDELMAN, L. R. FRANK, T. J. BRADY, AND B. R. ROSEN, *Science* **230,** 946 (1985).
2. L. AXEL, *Am. J. Roentgenol.* **143,** 1157 (1984).

3. W. G. BRADLEY AND V. W. WALUCH, *Radiology* **154,** 443 (1985).
4. P. R. MORAN, *Magn. Reson. Imaging* **1,** 197 (1982).
5. A. ABRAGAM, "Principles of Nuclear Magnetism," p. 34, Oxford Univ. Press, New York, 1961.
6. O. C. MORSE AND J. R. SINGER, *Science* **170,** 440 (1970).
7. J. H. BATTOCLETTI, A. SANCES, JR., S. J. LARSON, S. M. EVANS, R. L. BOWMAN, V. KUDRAVCEV, AND J. J. ACKMANN, *Bio-Med. Eng. (London)* **10,** 12 (1975).
8. P. A. BOTTOMLEY, T. H. FOSTER, R. E. ARGERSINGER, AND L. M. PFEIFER, *Med. Phys.* **11,** 425 (1984).
9. S. H. KOENIG, R. D. BROWN, D. ADAMS, D. EMERSON, AND C. G. HARRISON, *Invest. Radiol.* **19,** 76 (1984).
10. R. L. EHMAN, J. P. FELMLEE, P. R. JULSRUD, AND J. E. GRAY, *Radiology* **157P** (special abstract edition), 121 (1985).
11. G. K. VON SCHULTHESS AND C. B. HIGGINS, *Radiology* **157,** 687 (1985).
12. "Guidelines for Evaluating Electromagnetic Exposure Risk for Trials of Clinical NMR Systems," John C. Villforth, Director, Bureau of Radiologic Health, Food and Drug Administration, Rockville, Md. 20857, February 12, 1982.